# Accepted Manuscript

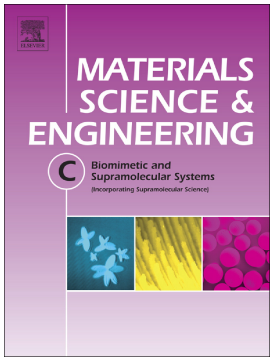


Nanocomposites based on pH-sensitive hydrogels and chitosan decorated carbon nanotubes with antibacterial properties

Romina Bellingeri, Lucinda Mulko, Maria Molina, Natalia Picco, Fabrisio Alustiza, Carolina Grosso, Adriana Vivas, Diego F. Acevedo, Cesar A. Barbero

PII: S0928-4931(17)33536-1
DOI: doi:10.1016/j.msec.2018.04.090
Reference: MSC 8547

To appear in: *Materials Science & Engineering C*

Received date: 14 September 2017
Revised date: 30 March 2018
Accepted date: 30 April 2018

Please cite this article as: Romina Bellingeri, Lucinda Mulko, Maria Molina, Natalia Picco, Fabrisio Alustiza, Carolina Grosso, Adriana Vivas, Diego F. Acevedo, Cesar A. Barbero , Nanocomposites based on pH-sensitive hydrogels and chitosan decorated carbon nanotubes with antibacterial properties. The address for the corresponding author was captured as affiliation for all authors. Please check if appropriate. Msc(2017), doi:10.1016/j.msec.2018.04.090

# Nanocomposites based on pH-sensitive hydrogels and chitosan decorated carbon nanotubes with antibacterial properties

Romina Bellingeri[1], Lucinda Mulko[2], Maria Molina[2], Natalia Picco[1], Fabrisio Alustiza[3], Carolina Grosso[1], Adriana Vivas[1], Diego F. Acevedo[4], Cesar A. Barbero[2]

[1] Universidad Nacional de Río Cuarto, Facultad de Agronomía y Veterinaria, Departamento de Anatomía Animal, Laboratorio de Biotecnología Animal, Ruta 36 km 601, Río Cuarto, Córdoba 5800, Argentina
[2] Universidad Nacional de Río Cuarto, Facultad de Ciencias Exactas, Físico-Químicas y Naturales, Departamento de Química, Laboratorio de Materiales Avanzados, Ruta 36 km 601, Río Cuarto, Córdoba 5800,
[3] Instituto Nacional de tecnología Agropecuaria (INTA). Estación experimental Marcos Juarez.
[4] Universidad Nacional de Río Cuarto, Facultad de Ingeniería, Departamento de Tecnología Química, Ruta 36 km 601, Río Cuarto, Córdoba 5800, Argentina

## Abstract

The present work aimed to study the properties of a novel nanocomposite with promising biomedical applications. Nanocomposites were prepared by the addition of different concentrations of chitosan decorated carbon nanotubes to acrylamide-co-acrylic acid hydrogels. The nanocomposites chemical structure was characterized by Fourier Transform Infrared Spectroscopy (FT-IR). The FT-IR shows the typical bands due to the hydrogel and additionally the peaks at 1750 $cm^{-1}$ and 1450 $cm^{-1}$ that correspond to the carbon nanotubes incorporated into the polymer matrix. Mechanical properties and swelling measurements in different buffer solutions were also performed. The nanocomposites showed improved mechanical properties and a stronger pH-response. In order to evaluate antimicrobial activity, the growth and adhesion of *Staphylococcus aureus* to nanocomposites were studied. Cytocompatibility was also evaluated by MTT assay on MDCK and 3T3 cell lines. The nanocomposites were found to be cytocompatible and showed a reduced bacterial colonization.

*Keywords*: biomaterials; chitosan; carbon nanotubes; pH-sensitive hydrogels; antimicrobial activity; nanocomposites

## Introduction

Bacterial infections are a leading cause of morbidity and mortality worldwide. Polymer nanocomposites have attracted considerable attention in recent years and have become key materials in modern nanotechnologies. They constitute a new alternative to conventionally filled polymers with significant biomedical potential. They can be defined as materials in which nanometer scaled materials are dispersed in polymer matrix in order to improve the structures and properties of the polymers [1]. Polymer nanocomposites can offer new opportunities for potential antibacterial treatment, tissues engineering, cancer therapy, medical imaging, dental applications, drug delivery, etc. [2]. Nanocomposites based on smart hydrogels and carbon nanotubes have been studied previously in the field of animal health and constitute an excellent strategy for the treatment of infectious diseases [3]. Smart hydrogels perceive the stimulus and respond by a change in their physical and/or chemical behavior leading to release of the entrapped drug [4]. On the other hand, functionalized carbon nanotubes (CNT) display unique properties that make them valuable filler to polymers, enable a variety of medicinal applications [5]. Many functionalization techniques have been developed in recent years to solubilize CNT, including the use of chitosan (CH), a polysaccharide synthesized from chitin, a biopolymer commonly isolated from the shells of marine crustacean, which are a waste of food

industry. Chitosan has several applications in biomedical fields such as wound dressing, artificial skin, nutrition, ophthalmology, drug delivery systems, tissue engineering due to its biocompatibility and biodegradability [6, 7]. Antibacterial activity of CH has been found in previous reports, where various Gram negative and Gram positive bacteria have been used [8].

In this study, we prepared different nanocomposites (NC) using a hydrogel based on a copolymer of acrylamide (AAm) and acrylic acid (AAc) as matrix and CH decorated CNT as reinforcement/modifier. The NC were characterized and their antimicrobial activity against *S. aureus* was studied. In addition, the cytocompatibility of NC was tested by MTT assay. The main goal of this work is to combine the pH responsive properties of the hydrogel with the antimicrobial activity of CH and the mechanical properties of CNT in order to fabricate a novel antimicrobial nanobiomaterial.

## MATHERIALS AND METHODS

### Carbon nanotubes

Multiwalled CNT (MWCNT) were obtained from Sun Nanotek Co. Ltd., China. They were synthesized by chemical vapor deposition, with 10–30 nm of diameter and 1–10 µm of length. The CNT have purity of 92% wt. The other impurities are iron of about 3% wt being in CNT soot in formation of $Fe_2O_2$, Al of 1% wt being in CNT soot in formation of $Al_2O_3$, and carbon black of 2% wt. The detect methods used for manufacturer included inductively coupled plasma mass spectrometry (ICP-MS) for Fe and Al contents and thermogravimetric analysis (TGA) for evaluation of CNT and carbon black. Before use, 2.5 g of multi walled CNT were oxidized in 26 mL of 3:1 molar ratio acid solution ($H_2SO_4$:$HNO_3$) for 3 h at 80 °C with magnetic stirring in order to purify them and to create the negatively charged groups on them. The acid treated CNT then were washed repeatedly with deionized water until a pH of the solution was neutral. Finally, the purified CNT were dried in vacuum oven for 24 h at 100 °C.

### *Decoration of CNT with CH*

Chitosan (CH ≥ 75% deacetylation, MW=100 kDa) was provided by Sigma-Aldrich®. Surface decoration of CNT with CH was done by dispersing 100 mg CNT in 100 mL CH solution (0.1 g CH dissolved in 100 mL 1% acetic acid solutions, pH 2). The mixture was treated under ultrasonic field for 10 min and then stirred for 1 h. During this step, CH macromolecules were adsorbed on the surface of the CNT thereby acting as polymer cationic surfactant to stabilize the CNT. A stable black suspension was obtained which indicates formation of a non-destroyable surface decoration/wrapping of carbon nanotubes with chitosan biopolymer.

### *Synthesis of hydrogel-CNT-CH composites*

The composites were synthesized according to previously reported methodologies [9]. AAm (Aldrich) and AAc (Aldrich) were used as monomers. The used cross-linker was N,N'-methylene bisacrylamide (BAAm, Roth). As redox initiator system ammonium persulfate (APS, Roth) and N,N,N',N'-tetramethyl ethylene diamine (TEMED, Merck) were used. Monomers and cross-linker were dissolved in distilled water, and then the solution was bubbled with nitrogen for 15 min. After that, a solution containing APS (0.001 g/mL) and TEMED (10 µL/mL) was added and the reaction mixture was sealed. The free radical polymerization of the hydrogels was carried out in tuberculin syringes at room temperature (22 °C) for 3 h. The extreme of the syringe was cut and the gel was expulsed and sectioned into similar pieces (5 mm). The resulting gels were washed several times with distilled water during one week to remove all the unreacted monomers. The pH of the

water was measured to verify that unreacted monomers were eliminated. Then, hydrogels were dried at room temperature until they reached constant weight. Three different types of composites were prepared: hydrogel, hydrogel-$(CNT\text{-}CH)_{1\%}$, hydrogel-$(CNT\text{-}CH)_{5\%}$ and hydrogel-$(CNT\text{-}CH)_{10\%}$. In the last three groups a percentage of water was replaced by a solution of CH-wrapped CNT (1.5 mg/mL). All samples were sterilized at 121 °C for 20 min in a pressurized steam autoclave before bacterial assays.

***Characterization***

*Swelling studies*

For the pH dependent swelling studies, hydrogels were incubated in buffer solutions ranging from pH 2.2 to 10, at room temperature for 24 h.

Table 1: Buffer solution used for swelling studies

| pH | Buffer |
|---|---|
| 2.2 | KCl/HCl (0.2 M) |
| 5.5 | NaOAc /HOAc (0.2 M) |
| 7.4 | $NaOH/KH_2PO_4/Na_2HPO_4$ (0.1 M) |
| 8 | Na2HPO4/NaH2PO4 (0.2 M) |
| 10 | $NaHCO_3$/NaOH (0.1M) |

After 24 h, the hydrogels were withdrawn from the buffer solution, measured, and weighed after removal of excessive surface water by lightly blotting with a filter paper. The swelling percentage was calculated by using the following equation:

$$\mathbf{Sw\%} = \left[\frac{(Ws - Wd)}{Wd}\right] \times \mathbf{100} \qquad \text{(Equation 1)}$$

Where *Ws* and *Wd* represents the weight of the swollen and dry sample, respectively. The geometric mean of Sw% in each pH was compared with a non-parametric Kruskal-Wallis test.

*Porosity Test*

The porosity of hydrogels was measured by liquid displacement method as reported earlier [10]. Initially the volume of ethanol and dry weight of the hydrogels were measured. Then the hydrogels were immersed into the dehydrated alcohol until it was saturated by absorbing the alcohol and the hydrogels were weighed again. Finally, the porosity of the hydrogels was calculated with the following equation:

$$\mathbf{Porosity} = \frac{W_1 - W_3}{W_2 - W_3} \qquad \text{(Equation 2)}$$

Where $W_1$ is the initial known weight of ethanol, $W_2$ is the weight of sum of ethanol and submerged hydrogel sample and $W_3$ is the weight of ethanol after the removal of hydrogel sample.

*Mechanical Properties*

Mechanical elasticity curve for hydrogels with different loads of CNT-CH was studied. The modulus of elasticity was measured by application to a cylinder shape hydrated sample a

constant compressive force (σ) from its relaxed state until full compression against the degree of elastic deformation (ε) attained, according to Equations 3 and 4.

$$\boldsymbol{\sigma} = \frac{\boldsymbol{F}}{\boldsymbol{A}} \quad \text{(Equation 3)}$$

$$\varepsilon = \frac{\Delta L}{L} = \frac{L_n - L}{L} \quad \text{(Equation 4)}$$

Where: *F, A, L* and $L_n$ are the compressive force, cross sectional area, final, and initial length of the hydrogel cylinder, respectively. The slope of the graph σ vs. ε is the Young's modulus or modulus of elasticity (E). All measurements were performed at standard conditions for temperature and pressure.

*Fourier transform infrared (FT-IR) spectroscopy*

Fourier Transform Infrared Spectroscopy measurements were recorded in ATR mode from 600 to 4000 $cm^{-1}$ with a resolution of 4 $cm^{-1}$ on a FT-IR Perkin Elmer (Model Spectrum Two). Device was equipped with a DynaScan interpherometer. Software used as interface was Spectrum 10.

***Antimicrobial Activity***

*Bacterial culture*

Cells of *Staphylococcus aureus* (*S. aureus*) (ATCC 29213) were culture in Trypticase Soy Broth (TSB, Britania Laboratory, Ref. B0410361, Argentina) in 24-wells plate at 37 °C. The concentration of microbe solution was adjusted to give an initial optical density (O.D.) reading of approximately 0.07 at 600 nm wavelength on a microplate reader (Biolatin, Venezuela), which corresponds to the concentration of McFarland 1 solution (3 x $10^8$ CFU/mL).

*Bacterial Growth assay*

The bacterial growth assay was realized following Shahi *et al.*, [11] with minor modifications. Nanocomposites (0.1 g) and 20 mL of sterile 0.9 % NaCl solution were placed in 50 mL conical flask with cotton stopper, and the polymers were left to swell for 24 h. After that, the NaCl solution which was not absorbed was removed and 0.1 mL of the cell suspension was added to the flask. The mixture was continually shaken at 37 °C at 150 rpm. At 24 h, 0.5 mL of the cell suspension was pipetted out from the container, quickly mixed with 4.5 mL of sterilized physiological saline, and then decimal serial dilutions were prepared. The colonies were counted after inoculation at 37 °C for 24 h. Blank test was similarly conducted without polymer. Finally, the growth of the bacteria after 24 h in the presence and absence of nanocomposites was compared.

*Bacterial adhesion assay*

After 24 h of incubation with nanocomposites, adherent bacteria were detached by sonication for 10 min in 1 mL of TSB, followed by vortexing for 2 min, using a modification of the method of Barth *et al*. [12]. Total numbers of bacteria were determined by serial dilutions of 1:$10^4$ to 1:$10^8$ on Trypticase soy agar (TSA) plates; the plates were incubated at 37 °C for 24 h, and colonies counted. Numbers of released bacteria were calculated, based on dilution, and expressed as a function of nanocomposites weight.

**Cell viability assay**

*Cell culture*

Hydrogels were initially hydrated in PBS with antibiotic-antimycotic and then were washed in sterile PBS. Finally, gels were hydrated with complete cell culture medium (DMEM, 10% of bovine fetal serum (BFS) and antibiotic-antimycotic) overnight and placed at the bottom of cell culture dishes. MDCK (Madin Darby Canine Kidney) and 3T3 (derived from embryo fibroblast of Mus musculus) cell lines were employed to evaluate biocompatibility. Briefly, cells were trypsinized and seeded on multiwall plates at a density of 105 cells/well in a 24-well plate. The cells were incubated at 37 °C in a humidified atmosphere of 5% $CO_2$ in air. The morphology of cells was observed in an inverted microscope (Zeizz, Germany).

*MTT assay*

To evaluate the effect of hydrogels on cell viability the MTT assay was employed. The assay measures the conversion of 3-(4,5-dimethylthiazol-2-yl)- 2,5-diphenyltetrazolium bromide (MTT) to an insoluble formazan. The formazan was then solubilized, and the concentration was determined by spectrophotometer at 540 nm of optical density [13]. Briefly, MDCK and 3T3 cell lines were seeded in a 96-well plate at a density of 5000 cells/well in 100 µL of complete DMEM. The cells were allowed to grow in contact with different hydrogels with CNT (0%, 1%, 5%, 10%) for 24 h in an incubator at 37 °C in a humidified atmosphere of 5% CO2. Each experimental condition was run in quintupled, viability control group (in which the hydrogel was omitted) was included. After 4, 24 and 48 h of culture, the MTT reagent (5 mg/mL) was added to each well and further incubated for 3 h at the same temperature. The reaction mixture was removed from each well and replaced by 100 µL of dimethyl sulfoxide (DMSO). The absorbance (A) at 540 nm was measured using a microplate reader (Labsystem Multiscan MS®). The data are shown as mean value ± SD (standard deviation).

**Statistical analysis**

Data were analyzed with InfoStat version 2011 software [14]. ANOVA and a *posteriori* Tukey test and LSD Fisher test were made. Non-parametric Kruskal Wallis test was used. Statistical differences were considered by $p<0.05$.

## RESULTS

***Characterization of nanocomposites***

*Swelling percentage*

The swelling kinetics of nanocomposites incubated for 24 h in buffers with different pH was done to study pH-responsive properties (Figure 1). The swelling percentage of the bare hydrogel incubated at pH 2.2 was significantly higher compared with hydrogel-(CNT-CH) nanocomposites ($p<0.05$). A gradual increase on swelling ratio can be observed.

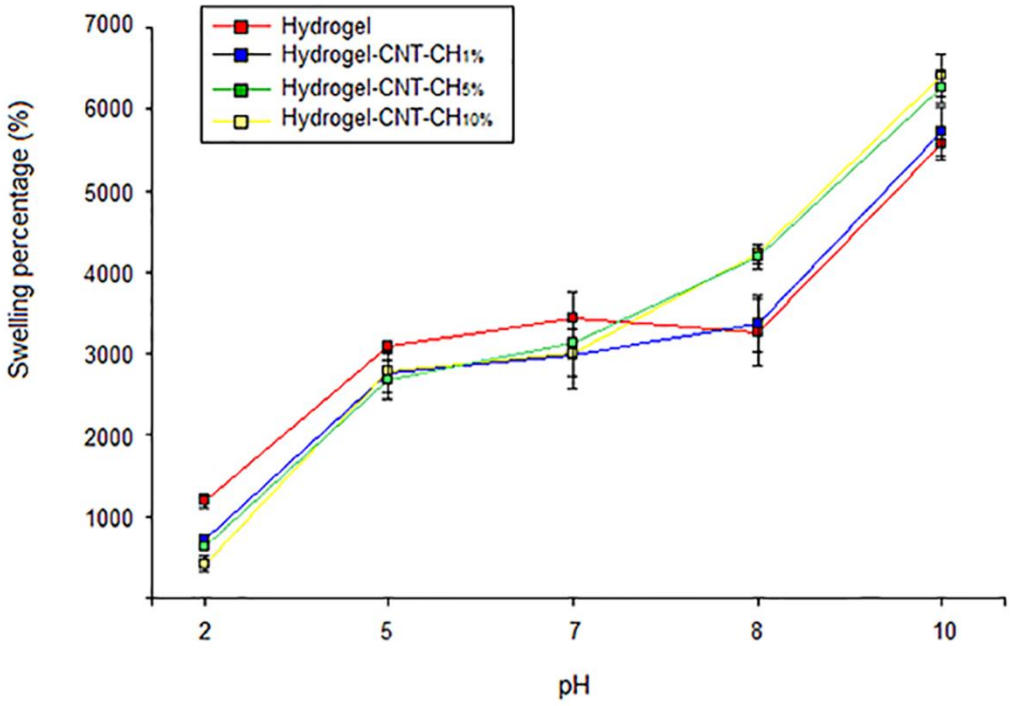


**Figure 1.** Influence of pH on swelling percentage of the nanocomposites. The values are mean (n = 3) ± SD.

*Porosity test*

The total porosity of the nanocomposites was estimated using liquid displacement method (Fig. 2); porosity of bare hydrogel was high (92.66%) and with the highest content of CH wrapped CNT in the polymeric matrix, the porosity was found to be significantly increased to 96.38% ($p \leq 0.05$). This increment may be probably due to the inhomogeneities caused by the presence of the CNT during the formation of the network.

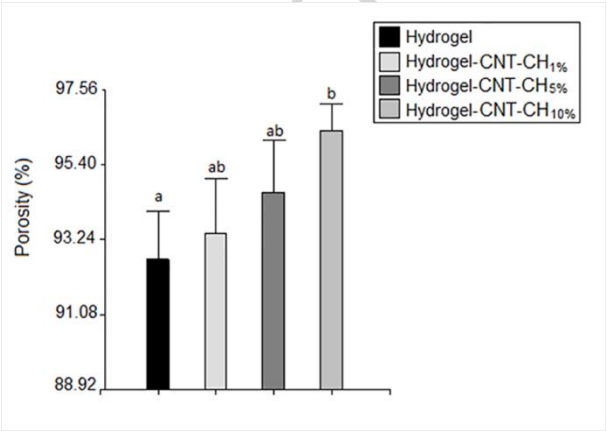


**Figure 2.** Porosity of hydrogel-(CNT-CH) composites after 48 h determined by the liquid displacement method, the values are mean ± SD (n = 3). Different letters indicate significant differences ($p \leq 0.05$). Kruskal–Wallis Test, Infostat, 2011.

*Mechanical properties*

Figure 3 shows the modulus of elasticity of the composites with different CNT content. The behavior of nanocomposites changes from elastic, for low loads of CNT (hydrogel-$CNT_{1\%}$) that is similar to pure acrylamide hydrogel, towards a more rigid and resistant to compression hydrogel for higher loads (hydrogel-$CNT_{5\%}$, hydrogel-$CNT_{10\%}$). The young module calculated from the stress strain curve is shown in Table 2.

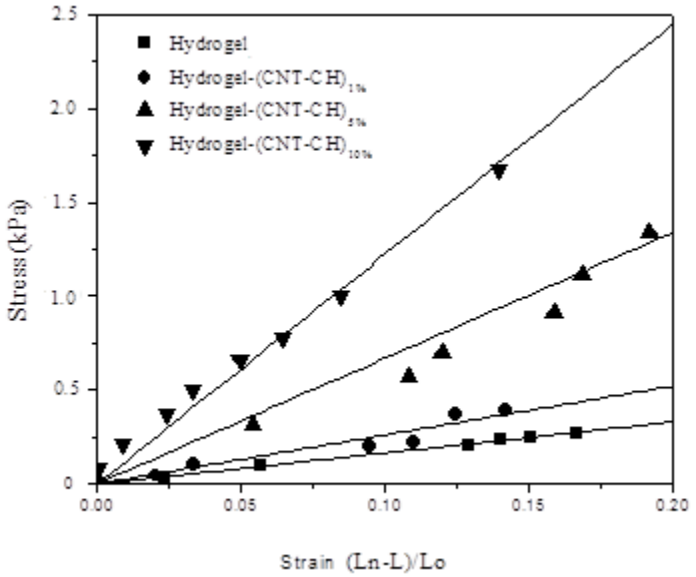


**Figure 3.** Modulus of elasticity (Young´s modulus) values of different samples. The data are presented as mean ± SD (n = 3).

Table 2. Young module oh hydrogel-CNT nanocomposites

| Materials | Young module (kPa) ± 0.200 |
|---|---|
| Hydrogel | 0.95 |
| Hydrogel-(CNT-CH)1% | 1.64 |
| Hydrogel-(CNT-CH)5% | 5.17 |
| Hydrogel-(CNT-CH)10% | 11.15 |

*Fourier transform infrared (FT-IR) spectroscopy*

To further characterize the obtained composites, FT-IR studies were conducted, the results are shown in Figure 4. In the FT-IR spectrum of bare hydrogel it is possible to observe the broad band at 3.437 $cm^{-1}$ corresponding to N-H stretching of the secondary amides. Also, bands at 2.974 and 2.881 $cm^{-1}$ are assigned to the $–CH_3$ symmetric and asymmetric stretching. The band at 1.670 $cm^{-1}$ is due to the C=O stretching vibration of the amide I band. The amide II band that appears at 1.576 $cm^{-1}$ is attributed to the N-H bending motion. On the FTIR spectra of the composites it is possible to observed the bands of the bare hydrogel and two characteristics peaks at 1750 $cm^{-1}$ and 1450 $cm^{-1}$ that correspond to the oxidized species of CNT. It is clearly seen that these new bands are concentration dependent, thus showing an increment with increasing amounts of CNT.

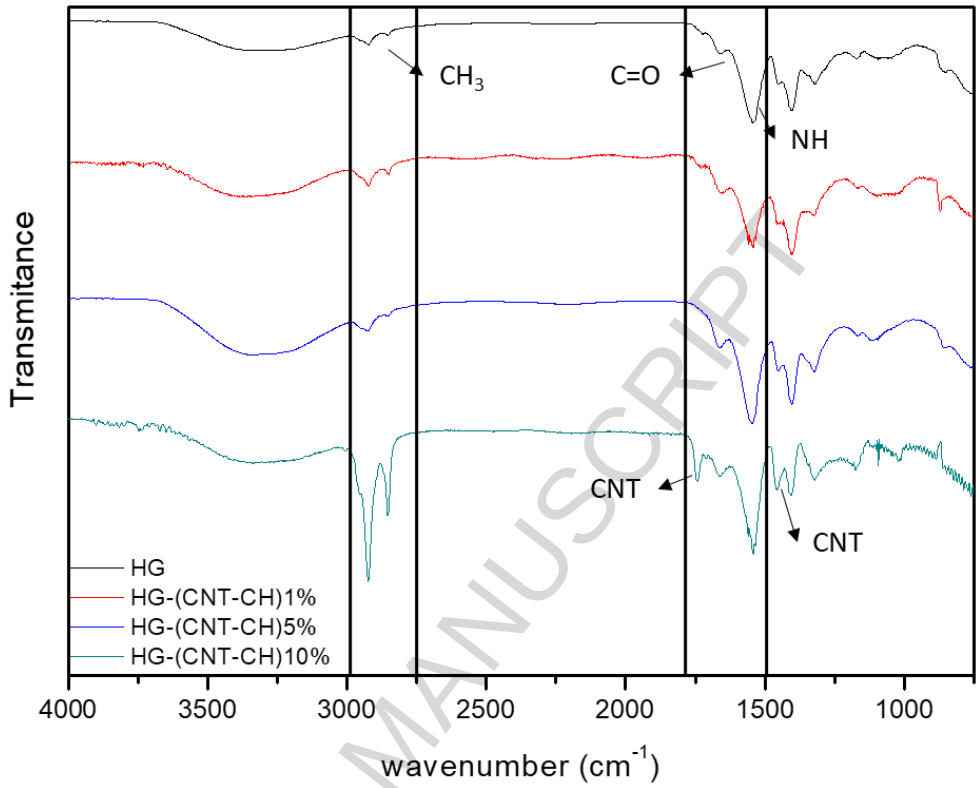


**Figure 4.** FT-IR spectra of bare hydrogel (HG), hydrogel-(CNT-CH)$_{1\%}$, hydrogel-(CNT-CH)$_{5\%}$, hydrogel-(CNT-CH)$_{10\%}$.

**Viability assay**

Related to viability, tested by MTT assay, not differences between positive control groups and cells exposed to hydrogels were detected. The assay was performed with two different cell lines and in both cases the results are the same. To corroborate acute or chronic toxic effect; the times of exposition were 4, 24 and 48h; not toxic effects were observed in those times. Moreover, not morphological changes were observed (Table 3).

Table 3. Cell viability percentage determined by MTT assay

| Cell line | Time of exposition | Positive Control | Hydrogel | Hydrogel CNT-CH$_{1\%}$ | Hydrogel CNT-CH$_{5\%}$ | Hydrogel CNT-CH$_{10\%}$ |
|---|---|---|---|---|---|---|
| MDCK | 4 h | 100 ± 0.9 | 100 ± 1.0 | 102 ± 1.2 | 105 ± 1.4 | 107 ± 2.1 |
| | 24 h | 100 ± 1.0 | 101 ± 1.2 | 100 ± 1.1 | 100 ± 1.2 | 100 ±1.7 |
| | 48 h | 100 ± 1.0 | 99 ± 0.9 | 100 ± 1.1 | 103 ± 0.9 | 102 ±1.7 |
| 3T3 | 4 h | 100 ± 0.9 | 101 ± 0.9 | 102 ± 1.0 | 102 ± 1.3 | 108 ±1.2 |
| | 24 h | 100 ± 0.9 | 100 ± 1.0 | 101 ± 0.9 | 100 ± 1.1 | 105 ±1.2 |
| | 48 h | 100 ± 0.9 | 101 ± 1.1 | 101 ± 1.2 | 104 ± 1.5 | 105 ±1.6 |

Date represents media (n=3) ± standard deviation (SD). Kruscal Wallis test, Infostat, 2011.

**Antimicrobial activity**

Table 4 shows the effect of nanocomposites on the growth of *S. aureus* ATCC 29213. The bacterial growth at 24 h shows no significant differences between nanocomposites, bare hydrogel, and control conditions.

Table 4. Antimicrobial activity evaluation of nanocomposites to *S. aureus* ATCC 29213.

| | Viable bacterial cells (Log CFU/mL) | Bacterial cells adhered (Log CFU/mL) |
|---|---|---|
| Control | $9.33 \pm 8.02^{a}$ | - |
| Hydrogel | $9.29 \pm 7.53^{a}$ | $7.89 \pm 6.49^{b}$ |
| Hydrogel-$(CNT\text{-}CH)_{1\%}$ | $9.26 \pm 8.02^{a}$ | $7.45 \pm 6.70^{b}$ |
| Hydrogel-$(CNT\text{-}CH)_{5\%}$ | $9.27 \pm 8.05^{a}$ | $4.38 \pm 3.62^{a}$ |
| Hydrogel-$(CNT\text{-}CH)_{10\%}$ | $9.26 \pm 7.88^{a}$ | $3.81 \pm 2.20^{a}$ |

Date represents media (n=3) ± standard deviation (SD). Different letter is indicative of statistical significance ($p<0.05$). Kruscal Wallis test, Infostat, 2011.

The amount of viable cells shows little effect of the presence of hydrogels and nanocomposites. The amount of cell adhered is very large in the hydrogel while it decreases sharply when the nanocomposites contains 5 or 10 % of CNT-CH.

**Discussion**

Better understanding of the interaction between microorganisms and biomaterials may improve our current approach to the treatment of infections. In order to obtain antibacterial polymeric nanocomposites, CH wrapped CNT were incorporated into pH-sensitive hydrogels. In our previous study, we have shown that the addition of CH wrapped CNT to the hydrogels improved the properties of these nanocomposites without affecting their biocompatibility [9] offering new opportunities for the treatment of certain infectious diseases [3, 15]. In this work, we prepared hydrogel-(CNT-CH) nanocomposites that were characterized and checked for antimicrobial activity against *S. aureus.*

The problem of poor dispersion of CNT can be improved by some pretreatment method such as functionalization with strong acid that generate carboxyl groups on their surfaces. [16]. Previous studies have shown that by creating defects on the sidewalls of CNT by an oxidative process, groups are generated that allow a better interaction with the CH [17]. In this work, we treated the CNT with nitric acid to favor the subsequent decoration of CNT with CH. Despite CH constitute a potential dispersing agent for CNT it could affect the mechanical properties of the final composite including the morphology and thickness of polymer. It is critical to tailor their structures and properties in many potential applications, which is significantly influenced by interfacial interactions between nanotubes and polymer matrices [18]. The remarkable mechanical properties of CNT make them the most ideal and promising reinforcements in substantially enhancing the mechanical properties of resulting polymer/CNT composites [19]. The results of this work showed that 1 % of CNT added in the polymer matrix resulted in 20 % increases in elastic modulus. Previous studies evaluated how the stiffness of a polymer hydrogel influences the initial attachment of bacteria and found that more *Escherichia coli* and *S. aureus* adhere to stiffer hydrogels and that this relationship occur independent of hydrogel chemistry [20]. We found that *S. aureus* adhere more to soft (hydrogel) and intermediate (hydrogel-$(CNT\text{-}CH)_{1\%}$) composites than the stiffer ones (hydrogel-$(CNT\text{-}CH)_{5\%}$ and hydrogel-$(CNT\text{-}CH)_{10\%}$).

The effect of the aspect ratio of CNT on the elastic properties of the nanocomposites and the interfacial region between nanotubes and the polymer matrix needs further study. Chae and Huang [21] used molecular dynamics simulations to perform a systematic study

on the mimetic synthesis, structural characterization, and mechanical properties of aligned CNT nanocomposites. It allows identifying the optimal synthesis parameters for desired structure and properties.

The swelling studies showed the regular swelling mechanism of anionic networks. At pH 2.2, the pH value of the surrounding medium is less than the pka and the carboxyl groups are non ionized. As a result, the mesh was in a collapsed state. On the contrary, at high pH the electrostatic repulsion between the negatively charged carboxyl groups generated the swelling of the hydrogel network [4]. The addition of significantly reduced the swelling in acidic conditions. Nanocomposites with 5 and 10% of CNT-CH show a higher swelling percentage in buffer solution with pH 8 and 10. Sensitivity to pH is an important property for transdermal delivery systems.

The porosity of nanocomposites significantly increases with the addition of CNT. Studies with functionalized CNT-based alginate hydrogels reveals a proportionately increment in pore sizes with increasing concentration of CNT. However, with increasing concentration of CNT, the gels became more brittle as evidenced by the cracks in the structures [22]. Some studies had the contrary effect and explain that, when the content of CNT increased the pore walls size is reduced maybe due to the increased viscosity of the blend solution [23]. Porosity parameters are important to determine the functionality of the nanocomposite, usually the higher the porosity the lower the mechanical strength. However, in this work the Youngs modulus increases with the addition of CNT as wells as the porosity.

Nanomaterials are an alternative to conventional antibiotic compounds, since they are unlikely to cause resistance in pathogen microorganisms [24]. However, a thorough knowledge of the mode of interaction of nanocomposites with bacteria at subcellular level is mandatory for any clinical application. The hydrogel-(CNT-CH) nanocomposites had no effect on bacterial growth, nevertheless a reduced bacterial attachment was observed in hydrogel-$(CNT\text{-}CH)_{10\%}$. The surface properties of biomaterials determine the kind and strength of communications between the biological environment and the materials. The bacterial adhesion depends in part on the ability of cells to sense and respond to their environment, including the nature of the polymer surface [25]. Despite *S. aureus* is historically defined as a non-motile organism, recent studies show it engages in a behavior that is consistent with it being actively motile under certain conditions [26]. These motility mechanisms of all types play an important role in virulence and colonization. Probably, the nanoscale roughness created by the incorporation of CNT was an influencing factor for the adhesion of *S. aureus* to the nanocomposites [27].

The use of nanocomposites as delivery or antibacterial devices implies that the material not only has to prevent bacterial attachment, but also it has to be compatible to the cells. A very wide number of assay techniques can be used to evaluate cytotoxicity, in the present study the viable cell number was analyzed by MTT test on MDCK and 3T3 cell lines. This assay focuses on mitochondrial metabolism and specifically evaluates an enzyme function (dehydrogenases). The yellow tetrazolium salts are reduced to water-insoluble purple-blue formazan crystals that precipitate in the cytosol and that are then solubilized after the induction of cellular lysis by a surfactant, enabling the absorbance to be read at 540 nm. A reduction of cellular metabolic activity is accepted as an early indicator of cellular damage [28]. In this work no cytotoxic effect were observed after culture the cell lines in the presence of nanocomposites, these results suggest that all the nanocomposites under study are biocompatible. Similarly, pH sensitive hydrogels based on poly-acrylamide, poly-acrylic acid and chitosan also have been found cytocompatible [29, 30]. However, Povea *et al*., [31] found that some hydrogels showed cytotoxic effect after seven days presenting viability lower than 80% respect to the control. This could be related with the possible presence of residual monomer in these systems.

Despite the potential hazards of CNT has previously reported, toxicity evaluation of these materials has to be taken on a case-by-case study, because CNT cannot be regarded as a simple chemical substance [32]. In this work, CNT are shielded, in some way, by the polymer matrix. Moreover, the CH that covers CNT could be passivate their surface preventing further reactions.

Controlled swelling, mechanical resistance, and reduced bacterial colonization are the favorable achieved features of these nanocomposites. To the best of our knowledge, our present study adds novelty to this field, because this is the first report concerning the use of hydrogel-(CNT-CH) nanocomposites against *S. aureus*. We believe that further efforts are still needed to better clarify the mechanisms that alters the adhesion of *S. aureus* in the understanding of how CNT-based nanocomposites interact with microorganisms.

In addition to having adequate pH sensitive properties and good mechanical strength, the nanocomposites must also show acceptable biocompatibility. Previous studies with these composites showed no signs of cytotoxicity on primary culture of porcine enterocytes probably may be because hydrogel matrix provides a shielding effect to CNT [9].

## CONCLUSIONS

The developed hydrogel-(CNT-CH) composites exhibited better mechanical and pH sensitive properties compared with the bare hydrogel. Moreover, the hydrogel and nanocomposites show non-significant hemolytic activity. Since the nanocomposites carrying 5 and 10% of CNT-CH shows pH-dependent swelling these biomaterials can be tested in targeted drug delivery. However, greater success in treating infections could be achieved by materials exhibiting inherent resistance to bacterial attachment, as has been demonstrated using these nanocomposites. Bacterial adhesion is a multifaceted process affected by many factors, further studies are required to understand the mechanisms of bacterial adhesion and adequate methodologies to prevent and treat infectious diseases. The favorable cytocompatibility results for all the nanocomposites opens avenues for in vivo safety and efficacy studies for biomedical applications.

## ACKNOWLEDGMENTS

R. Bellingeri, D.F. Acevedo, M.A. Molina and C.A. Barbero are permanent fellows of CONICET. L. Mulko thanks CONICET for a graduate fellowship. This work was supported by grants from Agencia Nacional de Promoción Científica y Tecnológica (FONCYT- PICT N° 2014-0946), CONICET (PIP 2013-2015) and Secretaría de Ciencia y Técnica de la Universidad Nacional de Río Cuarto (SECYT-UNRC).

## CONFLICT OF INTEREST

The authors confirm that there are no known conflicts of interest associated with this publication and there has been no significant financial support for this work that could have influenced its outcome.

## REFERENCES

1. B. Arash, H.S. Park, T. Rabczuk, Mechanical properties of carbon nanotube reinforced polymer nanocomposites: a coarse-grained model. Compos. B Eng. 80 (2015) 92-100.
2. D. Feldman, Polymer nanocomposites in medicine. J. Macromol. Sci. A 53.1 (2016) 55-62.
3. F. Alustiza, R. Bellingeri, N. Picco, C. Motta, M.C. Grosso, C. Barbero, D. Acevedo, A. Vivas, IgY against enterotoxigenic Escherichia coli administered by hydrogel-

carbon nanotubes composites to prevent neonatal diarrhoea in experimentally challenged piglets. Vaccine 34 (2016) 3291-3297.
4. P. Gupta, K. Vermani, S. Garg, Hydrogels: From controlled release to ph-responsive drug delivery. Drug Discov. Today 7 (2002) 569-579.
5. Y. Zhang, Y. Bai, B. Yan, Functionalized carbon nanotubes for potential medicinal applications. Drug Discov. Today, 15.11-12 (2010) 428-435.
6. R.C.F. Cheung, T.B. Ng, J.H. Wong, W.Y. Chan, Chitosan: an update on potential biomedical and pharmaceutical applications. Mar. drugs 13.8 (2015) 5156-5186.
7. J. Venkatesan, I. Bhatnagar, S.K. Kim, Chitosan-alginate biocomposite containing fucoidan for bone tissue engineering. Mar. drugs 12.1 (2014) 300-316.
8. M.S. Benhabiles, R. Salah, H. Lounici, N. Drouiche, M.F.A. Goosen, N. Mameri, Antibacterial activity of chitin, chitosan and its oligomers prepared from shrimp shell waste. Food Hydrocoll. 29 (2012) 48-56.
9. R. Bellingeri, F. Alustiza, N. Picco, D. Acevedo, M.A. Molina, R. Rivero, C. Grosso, C. Motta, C. Barbero, A. Vivas, In Vitro Toxicity Evaluation of Hydrogel–Carbon Nanotubes Composites on Intestinal Cells. J. Appl. Polym. Sci. 132.5 (2015) 1-7.
10. J. Venkatesan, B. Ryu, P.N. Sudha, S.K. Kim, Preparation and characterization of chitosan-carbon nanotube scaffolds for bone tissue engineering. Int. J. Biol. Macromol. 50 (2012) 393-402.
11. S. Shahi, M.J. Zohuriaan-Mehr, H. Omidian, Antibacterial superabsorbing hydrogels with high saline-swelling properties without gel blockage: Toward ideal superabsorbents for hygienic applications. J. Bioact. Compat. Polym, 32.2 (2017) 128-145.
12. E. Barth, Q.M. Myrvik, W. Wagner, A.G. Gristina, In vitro and in vivo comparative colonization of Staphylococcus aureus and Staphylococcus epidermidis on orthopaedic implant materials. Biomaterials 10 (1989) 325-328.
13. van Meerloo J., Kaspers G.J.L., Cloos J. (2011) Cell Sensitivity Assays: The MTT Assay. In: Cree I. (eds) Cancer Cell Culture. Methods in Molecular Biology (Methods and Protocols), vol 731. Humana Press
14. J.A. Di Rienzo, F. Casanoves, M.G. Balzarini, L. Gonzalez, M. Tablada, Y.C. Robledo (2011) InfoStat versión 2011. Grupo InfoStat, FCA, Universidad Nacional de Córdoba, Argentina. URL http://www. infostat. com. ar.
15. R. Bellingeri, F. Alustiza, N. Picco, C. Motta, M.C. Grosso, C. Barbero, D. Acevedo, A. Vivas, Hydrogel–Carbon Nanotubes Composites for Protection of Egg Yolk Antibodies. In: A. Tiwari, Y.K. Mishra, H. Kobayashi, A.P.F. Turner (Eds.), Smart Nanocomposites, Fabrication, and Applications. Intelligent Nanomaterials, 2nd edition, John Wiley & Sons, 2016, pp 515-546.
16. K. Balasubramanian, M. Burghard, Chemically functionalized carbon nanotubes. Small 1 (2005) 180-192.
17. K. Esumi, M. Ishigami, A. Nakajima, K. Sawada, H. Honda, Chemical treatment of carbon nanotubes. Carbon 34.2 (1996) 279-281.
18. S. Lee, B. Kim, S. Chen, Y. Shao-Horn, P. Hammond. Layer-by-layer assembly of all carbon nanotube ultrathin films for electrochemical applications. J. Am. Chem. Soc. 131 (2009) 671-679.
19. B. Arash, Q. Wang, V.K. Varadan, Mechanical properties of carbon nanotube/polymer composites. Sci Rep 4 (2014) 6479. http://doi.org/10.1038/srep06479
20. K.W. Kolewe, S.R. Peyton, J.D. Schiffman, Fewer Bacteria Adhere to Softer Hydrogels. ACS Appl. Mater. Interfaces 7.35 (2015) 19562-19569.

21. K. Chae, L. Huang, Computational Study of Pressure-Driven Gas Transport in Nanostructured Carbons: An Alternative Approach. J. Phys. Chem. B *119*.37 (2015) 12299-12307.
22. B. Joddar, E. Garcia, A. Casas, C.M. Stewart, Development of functionalized multi-walled carbon-nanotube-based alginate hydrogels for enabling biomimetic technologies. Sci. Rep. 6 (2016) 32456. Doi:10.1038/srep32456.
23. V. Vatanpour, S.S. Madaeni, R. Moradian, S. Zinadini, B. Astinchap, Fabrication and characterization of novel antifouling nanofiltration membrane prepared from oxidized multiwalled carbon nanotube/polyethersulfone nanocomposite. J. Membr. Sci. 375.1 (2011) 284-294.
24. A.J. Huh, Y.J. Kwon, Nanoantibiotics: a new paradigm for treating infectious diseases using nanomaterials in the antibiotics resistant era. J. Control Release. 156.2 (2011) 128-45.
25. A.L. Hook, C.Y. Chang, J. Yang, J. Luckett, A. Cockayne, S. Atkinson, M.R. Alexander, Combinatorial discovery of polymers resistant to bacterial attachment. Nature Biotech 30.9 (2012) 868-875.
26. E.J. Pollitt, S.A. Crusz, S.P. Diggle, Staphylococcus aureus forms spreading dendrites that have characteristics of active motility. Sci. Rep. 5 (2015) 17698.
27. G. Bhardwaj, T.J. Webster, Reduced bacterial growth and increased osteoblast proliferation on titanium with a nanophase TiO2 surface treatment. Int. J. Nanomedicine 6.12 (2017) 363-369.
28. J. van Meerloo, G.J.L. Kaspers, J. Cloos, Cell Sensitivity Assays: The MTT Assay. In: Cree I. (eds) Cancer Cell Culture. Methods in Molecular Biology (Methods and Protocols), vol 731. (2011) Humana Press.
29. M.V. Risbud, R. R. Bhonde, Polyacrylamide-Chitosan Hydrogels: In Vitro Biocompatibility and Sustained Antibiotic Release Studies. Drug Delivery, 7.2 (2000) 69-75, DOI: 10.1080/107175400266623.
30. P. Ghorbaniazar, A. Sepehrianazar, M. Eskandani, M. Nabi-Meibodi, M. Kouhsoltani, H. Hamishehkar, Preparation of Poly Acrylic Acid-Poly Acrylamide Composite Nanogels by Radiation Technique. Adv Pharm Bull, 5.2, (2015) 269-275.
31. M.B. Povea, W.A. Monal, J.V.C. Rodríguez, A.M. Pat, N.B. Rivero, C.P. Covas, Interpenetrated Chitosan-Poly(Acrylic Acid-Co-Acrylamide) Hydrogels. Synthesis, Characterization and Sustained Protein Release Studies. Mater Sci Appl 2 (2011) 509-520.
32. H. Meng, T. Xia, S. George, A.E. NelA predictive toxicological paradigm for the safety assessment of nanomaterials. ACS Nano 3 (2009) 1620-1627

**Highlights**

- A novel nanocomposite with promising biomedical applications was produced and characterized
- The FT-IR shows the typical bands due to the hydrogel and additionally the peaks at that correspond to the carbon nanotubes incorporated into the polymer matrix.
- The nanocomposites showed improved mechanical properties and a stronger pH-response compared with bare hydrogel.
- The nanocomposites were found to be cytocompatible and showed a reduced bacterial colonization.